

A proposal for Common-opening-angle Migration/Inversion

Norman Bleistein¹ and Samuel H. Gray²

Abstract

We derive a Kirchhoff migration-inversion technique as an integral over migration dip at an output point at depth. In this method, the opening angle between rays from source and receiver are constrained to make a fixed angle at the output point. Thus, this is a common angle migration-inversion, in contrast to the more standard common-offset or common shot methods. This method has the advantage of dealing more routinely with multipathing of rays than do those latter two methods. Previous derivations of this method use the generalized Radon theory and pseudo-differential operator/Fourier integral operator theory or use least squares methodology. Thus, the results are not new—although some of the formulas are. The derivation here arises from more classical Kirchhoff modeling and inversion theory, hopefully more accessible to the geophysical community. Further, it demonstrates that this migration-inversion method is an alternative Kirchhoff method for a different sorting of the data.

1 Introduction

This paper presents a classical derivation for Kirchhoff migration-inversion in dip for common opening angle between source and receiver rays. Migration dip is the direction of the gradient of the total travel time function from source and receiver points to the image point in the background wave speed medium. The method treats multipathing of rays between surface and depth points in a more routine manner than do standard common shot or common-offset methods. We derive the method as an integration over migration dip at the image point, in contrast to the integration over the surface trace coordinates in the aforementioned methods. Xu, et al., [2001] demonstrate, however, that one can also carry out the integration over sources and receivers with a windowing criterion that fixes the opening angle of the rays at the output point. Thus, the more familiar common-offset output panels are replaced by common opening angle output panels. See Figure 1 for the relevant variables in 2D. In this figure, the unit vector $\hat{\nu}$ points in the direction of the gradient of the sum of travel times from source and receiver; ϕ denotes the angle that $\hat{\nu}$ makes with the vertical, and defines the

¹Center for Wave Phenomena, Colorado School of Mines, Golden, CO 80401-1887 USA

²Veritas DGC Inc., 715 Fifth Avenue SW, Suite 2200, Calgary, AB T2P 5A2, Canada

dip direction. Thus, we are proposing an integration over ϕ in our Kirchhoff inversion. The angles between $\hat{\alpha}_r$ or *ashat* and the dip vector is denoted θ , in which case, 2θ is the common opening angle between the rays. Note that this depiction is for an isotropic background medium; for anisotropic media, the dip direction does not, in general, make equal angles with the two ray directions. We treat only the case of a constant density acoustic medium in this paper.

Since common opening angle at depth does not translate into common-offset at the surface, the method requires access to a suite of common-offset panels for each output summation. The method also requires that rays, travel times and other ray quantities be computed from points at depth rather than from points at the upper surface. However, we show how integration over dip can be transformed back into a sum over sources and receivers at the upper surface. This transformation, then, relates our results back to those of Xu, et al., [2001].

The advantages of this method are as follows.

1. The Beylkin determinant—an important factor in the inversion process—is constant in dip inversion, thus simplifying the computation, in particular, avoiding the common-offset calculation of the Beylkin determinant in 3D.
2. The output is a reflectivity map at known (constant) specular angle, since that angle is an input variable for each computation.
3. The peak amplitude of the output is proportional to the reflection coefficient at that opening angle, with known scale factor. Thus, an AVA moveout plot is easily computed from the peak amplitudes.

This type of processing was proposed in de Hoop, et al. [1994], with follow-on discussions in de Hoop [1998] and de Hoop and Brandsberg-Dahl [2000]. The presentation of de Hoop and Brandsberg-Dahl requires implementation of the generalized Radon transform technique and an understanding of pseudo-differential/Fourier integral operators. Further, they present formulas for only the most general anisotropic elastic cases, from which it is difficult to produce simpler results.

Xu et al. [2001] derive the acoustic result using the least-squares approach; the type of processing we derived here is their first iterate. Their results are presented in 2D. They state the formula for dip inversion as a sum over sources and receivers. The corresponding formula for summation over dip requires just a one-line derivation to deduce this formula from their equations (33-35). Their equation (33) is a formula for model-perturbation update as an integration over dip; (34) is a formula for model perturbation as an integration over all sources and receivers; (35) is a formula for reflectivity as an integral over sources and

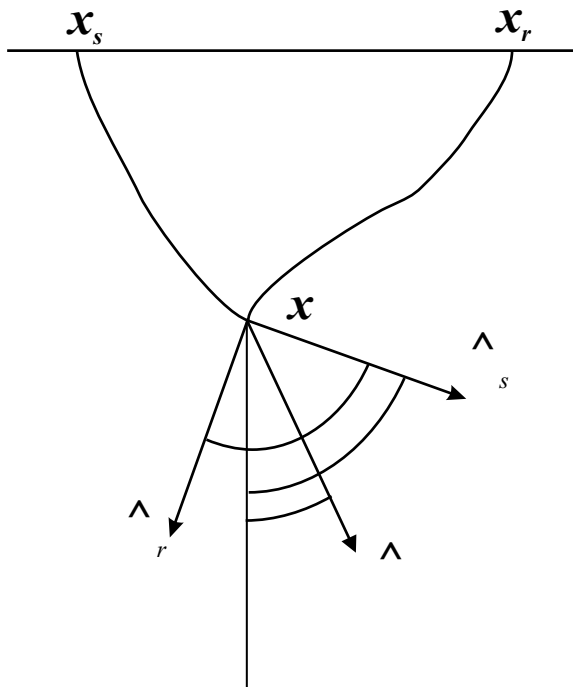


Figure 1: Angles of common opening angle Kirchhoff migration-inversion carried out as an integration over dip. $\hat{\nu}$, the unit vector in the direction of the sum of the gradients of the travel time; this vector defines the migration dip direction. ϕ , is the dip, the angle of $\hat{\nu}$ with respect to the vertical. $\hat{\alpha}_s$ is a unit vector in the direction of the ray from the source \mathbf{x}_s to the output point \mathbf{x} , and $\hat{\alpha}_r$ is a unit vector in the direction of the ray from the receiver \mathbf{x}_r to the output point \mathbf{x} . θ is the common opening angle between ϕ and α_s and also the angle between ϕ and α_r . Finally, $\alpha_s = \phi + \theta$; $\alpha_r = \phi - \theta$, are the angles that $\hat{\alpha}_r$ and $\hat{\alpha}_s$ make with the vertical.

receivers; our result is a formula for reflectivity as an integral over dip. In the integrals over sources and receivers, they use a window function to restrict the source-receiver pairs to those having approximately the right opening angle at the output point. (We use this trick, below, to derive the formulas for summation over sources and receivers from the derived formulas for summation over dip.) They also provide extensive numerical examples that demonstrate the value of using all arrivals in the presence of multipath trajectories. Their computer output was generated from the formula for model perturbation as an integral over sources and receivers.

What is new here is only a derivation based on more classical methods, namely the Kirchhoff inversion technique as described in Bleistein et al. [2001]. We believe that the present derivation is more accessible to a geophysical readership and further demonstrates that this is just a natural extension of the more classical method. This approach places

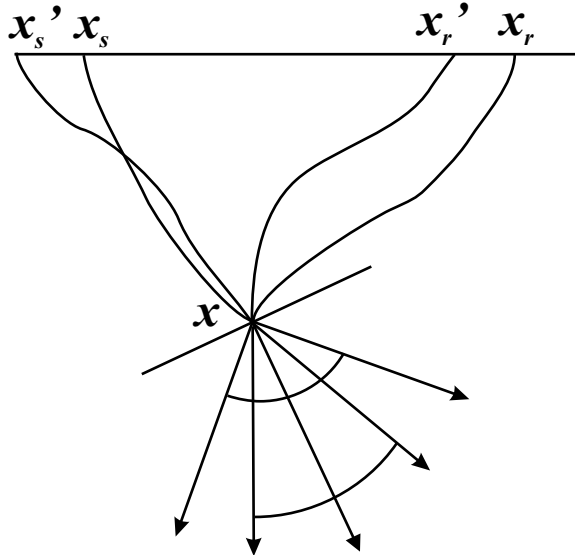


Figure 2: A dipping reflector with two sets of specular rays from the source-receiver pairs, \mathbf{x}_s , \mathbf{x}_r and \mathbf{x}'_s , \mathbf{x}'_r , respectively. They have the same offset, but different opening angles at depth.

migration-inversion as an integral over dip in the class of Kirchhoff formulas. Furthermore, the explicit statement of the formulas for the 3D and 2.5D acoustic cases are also new.

When multiple arrivals from a single subsurface location occur, common-offset migration-inversion processing typically picks up only one of these to add to the running sums that produce the output—perhaps the first arrival or the most energetic arrival. Picking up the contributions from multiple specular returns requires extra complexity in the migration program to force the sum to include all ray paths. This results in an output that is a sum over two or more specular terms wherever such multiple events occur, making amplitude studies problematic. Figure 2 shows two specular ray pairs for a point \mathbf{x} on a dipping reflector and for source-receiver pairs, \mathbf{x}_s , \mathbf{x}_r and \mathbf{x}'_s , \mathbf{x}'_r , respectively. Furthermore, these two pairs of rays have the same offset between source and receiver, but different opening angles at \mathbf{x} . The opening angles are indicated by the two arcs connecting the directions of the source and receiver rays for each pair at the specular point. A common-offset migration or inversion that uses only one arrival will pick up a contribution from only one or the other of these specular returns. A common-offset migration or inversion that uses multiple passes to pick up all returns will add the two outputs at the point \mathbf{x} .

Even when single specular returns produce an image at a point, the opening angle of the specular rays producing the output is unknown *a priori*. Thus, amplitude behavior must be resolved by further processing and analysis. In the approach of Bleistein, et al., [2001], two inversion formulas are processed; the quotient of the outputs at peak amplitude estimates the

opening angle between the specular rays and, hence, the angle of the angularly-dependent reflection coefficient. Although the different formulas for these inversions are minimal, it is necessary to retain two migrations or inversions in memory, pick peak amplitudes and take a quotient to estimate the cosine of the opening angle.

Common-opening-angle migration, carried out as a sum over all possible dips provides a better approach for dealing with these shortcomings. For the example of Figure 2, the processing will pick up both of these specular returns, but on different common-opening-angle panels. Hence, no summing of contributions from the two different specular arrivals occurs.

Common-opening-angle at depth does not translate into common-offset at the upper surface. We shoot rays from the output point at depth opposite to the directions of $\hat{\alpha}_s$ and $\hat{\alpha}_r$ of Figure 1. Their arrival points at the upper surface are the source and receiver locations, respectively. These, in turn, define the midpoint and offset of a trace. Thus, for each output point and half-opening angle θ , we must have access to traces in the range of offsets and midpoints defined by these arrivals. The same type of calculation is necessary for the Jacobians that arise in computing the Green's function. This is a shortcoming of common-opening-angle migration/inversion.

On the other hand, the Beylkin determinant that appears in the inversion formula becomes extremely simple in this case. For 2D or 2.5D implementations, for example,

$$|H| = \left[\frac{2 \cos \theta}{c(\mathbf{x})} \right]^2 \left| \frac{d\hat{\nu}}{d\alpha_1} \right|, \quad (1)$$

where α_1 is any parameter that defines the rotation of $\hat{\nu}$. Note that $|d\hat{\nu}/d\alpha_1|d\alpha_1 = ds$, differential arclength on the unit circle, which is where the endpoint of the vector $\hat{\nu}$ resides. If we set

$$\hat{\nu} = (\cos \phi, \sin \phi), \quad (2)$$

then the differentiation in (1) leads to

$$|H| = \left[\frac{2 \cos \theta}{c(\mathbf{x})} \right]^2 \left| \frac{d\phi}{d\alpha_1} \right|. \quad (3)$$

That is, the Beylkin determinant is the product of two factors. The first is a universal factor depending on the opening angle between the rays and the wave speed. The second one measures the rate of change of the dip with respect to the running parameter that labels the rays. This result remains true for both common-offset and common-shot inversion, with α_1 being the midpoint in a common-offset data set and the receiver location in a common-source data set.

As ϕ ranges over dip from $\pi/2$ to $-\pi/2$ at fixed θ , the source and receive locations at the upper surface are single valued. There might be caustics in the ray family from the output point to the upper surface, so trace midpoints might increase, then decrease, then increase again in a sequence that recur might as ϕ ranges over its domain. (This means that the inverse relationship from midpoint to dip is *multi-valued*.) However, since the reflector has a prescribed dip, only one choice of ϕ will produce a specular pair of rays on the upper surface. If the data traces contain arrivals in a range that includes this specular pair at an interior point of the range, then the output of the migration-inversion processing will be proportional to the reflection coefficient at the prescribed θ . That is, an image is obtained if the downward normal to the reflector at \mathbf{x} —the reflector dip—is in the interior of the range of migration dips for which is data exist; the migration dip that dominates the output is collinear with the normal to the reflector.

In contrast, recall that common-offset inversion with multiple passes on the acquisition surface can have multiple specular returns and thus uninterpretable amplitudes. As indicated by Figure 2, this can occur because common-offset traces can have more than one specular source-receiver pair at the same dip; the opening angle for these different specular events will be different.

In 3D, for a given trace location, data from more than one azimuth may be present for a given common-offset. Then, the domain of integration or summation could include integration over this azimuth, as well as integration over dip. Thus, where a simple common offset inversion is carried out as an integral or sum over midpoints—say, a 2D spatial integral for 3D processing—this inversion might add an additional integral over azimuth, as depicted in Figure 3. This type of upper surface Kirchhoff migration-inversion would be an integral over

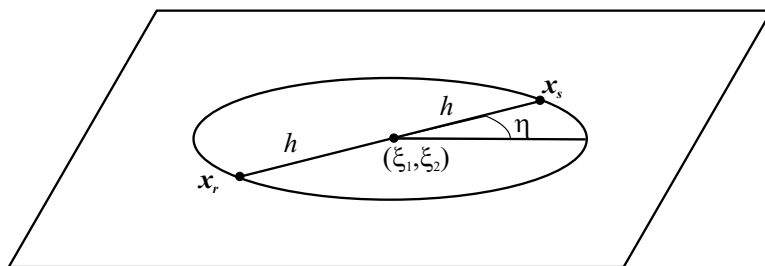


Figure 3: Location of a common offset source-receiver pair at midpoint, $\boldsymbol{\xi} = (\xi_1, \xi_2)$ and at azimuth η .

three spatial variables applied to data preprocessed with frequency domain filtering.

Figure 4 shows the coordinate system of interest for processing in common opening angle at depth. The vectors, $\hat{\boldsymbol{\alpha}}_s$ and $\hat{\boldsymbol{\alpha}}_r$ are unit vectors in the directions of the rays from source

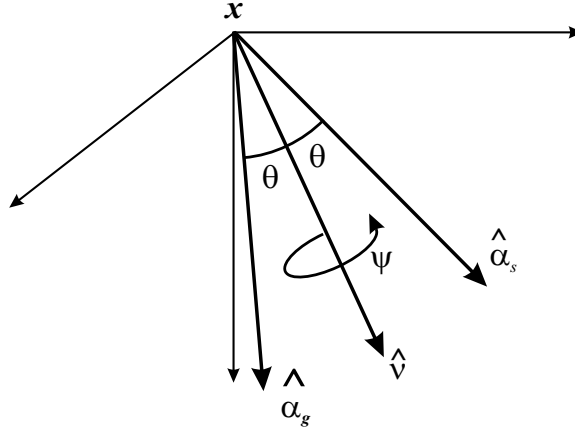


Figure 4: Coordinates for migration in dip characterized by $\hat{\nu}$, in azimuth ψ , and at fixed opening angle θ between rays to source and receiver. All are referenced to the output point \mathbf{x} . $\hat{\alpha}_s$ and $\hat{\alpha}_r$ are unit vectors in the directions of the rays from source and receiver, respectively. $\hat{\nu}$, $\hat{\alpha}_s$, and $\hat{\alpha}_r$ are in the same plane, so that the pair of vectors, $\hat{\alpha}_s$, and $\hat{\alpha}_r$, spin around $\hat{\nu}$ as ψ varies.

and receiver, respectively. The vectors, $\hat{\nu}$, $\hat{\alpha}_s$, and $\hat{\alpha}_r$, all lie in the same plane, also containing the output or imaging point, \mathbf{x} . If we think of shooting the rays back to the acquisition surface, their arrivals there are governed by the properties of the wave speed in the overburden. Their locations define a source-receiver pair and thereby defines a trace. It is not known *a priori* if the prescribed trace is included in the seismic survey. However, all nonzero traces defined in this manner contribute to the migration output at \mathbf{x} at the fixed opening angle θ . Thus, the final output for a given opening angle will be an average over the nonzero “hits” in source-receiver pairs at the upper surface. This might make sense for image enhancement in isotropic media, but would destroy amplitude information in anisotropic media. In that case, different azimuths would be treated separately and we would not carry out an integration in ψ . In the absence of this averaging step, the inversion formula is still valid. In any case, we derive the 3D result for an acoustic medium, where it makes sense to sum over azimuth, as well as dip. For migration purposes—say, to obtain a reflector map only—the amplitude could be simplified, thereby speeding up the computation. This simplification would preclude measuring reflection strength from the peak amplitude. However, the migration that results would still include multipath returns at common opening-angle.

2 3D Common Opening Angle Migration/Inversion in Dip Angle.

In this derivation, we follow the procedure of Bleistein, et al., [2001], Section 5.1.7. Thus, the objective is to determine the phase and amplitude of an integration kernel that will essentially invert the data to produce the reflectivity function. We should expect that this amplitude and phase will depend on all of the variables of the geometry introduced in Figure 4— $\mathbf{x}, \hat{\nu}, \theta, \psi$. and the frequency, ω . This inversion is carried out for the function $\beta(\mathbf{x})$.

2.1 The reflectivity function.

The derivation starts from a model of the observed wave field reflected from a single reflector whose surface will be denoted by S . We introduce the singular function of the reflector, $\gamma(\mathbf{x})$, which is a Dirac delta function, $\delta(s)$, of normal (signed) distance s from the reflector. Mathematically, distributions are defined by their “action” under integration on test functions. In this case,

$$\int_D \gamma(\mathbf{x})F(\mathbf{x})dV = \int_S F(\mathbf{x})dS. \quad (4)$$

Here, the domain D must contain the surface S . If one thinks of the volume integral as being carried out in the surface variables and s , then $dV = dS ds$. In this case, the action of the delta function, $\delta(s)$, on the left side integral is to evaluate the function $F(\mathbf{x})$ on S and to leave the surface integral yet to be done.

A graph of the support of the singular function is an image of the surface. A 3D “wiggle trace” plot or shade plot of a band limited version of the singular function is one type of image that we see in standard migration output. See Figure 5

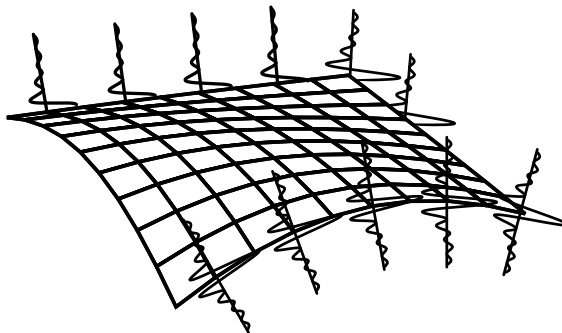


Figure 5: Wiggle trace depiction of the singular function of a surface.

The reflectivity function $\beta(\mathbf{x})$ is defined by

$$\beta(\mathbf{x}, \theta) = R(\mathbf{x}, \theta)\gamma(\mathbf{x}). \quad (5)$$

Here, R is the geometrical optics reflection coefficient at some incidence angle θ . In common-offset or common shot inversion, the choice of θ is problematic. Usually, it is disregarded in the definition of β . In those inversions or migrations, θ is determined *a posteriori* by various devices, depending on the nature of the inversion process. Two migrations or inversions are carried out in the Bleistein, et al., [2001], approach. Then the quotient of the peak amplitudes of these two results provides an estimate of $\cos\theta$ for a particular θ . That θ corresponds to the opening angle of a specular source-receiver pair for that output point on the reflector and for the given offset of the migration-inversion. In forward modeling via the Kirchhoff approximation written as a surface integral, θ is chosen to be the angle that the incident ray from the source makes with the normal to the reflector. After stationary phase analysis this turns out to be the specular incidence angle between rays from source and receiver point, with the stationary point in the variables of integration corresponding to the specular point on the reflector.

In any case, the method of stationary phase will ultimately bring all choices of θ to an appropriate specular choice. Thus, we will proceed with θ not being precisely defined at this point.

2.2 Forward modeling.

For forward acoustic modeling, we use the Kirchhoff approximation written as a volume integral as in Bleistein, et al., [2001], equation (5.1.54), to describe the observed wave field at a receiver \mathbf{x}_r due to a source at \mathbf{x}_s :

$$u(\mathbf{x}_s, \mathbf{x}_r, \omega) \sim -i\omega F(\omega) \int_D \beta(\mathbf{x}', \theta) a(\mathbf{x}', \mathbf{x}_s, \mathbf{x}_r) |\nabla\tau(\mathbf{x}', \mathbf{x}_s, \mathbf{x}_r)| \cdot e^{i\omega\tau(\mathbf{x}', \mathbf{x}_s, \mathbf{x}_r) - iK(\mathbf{x}', \mathbf{x}_s, \mathbf{x}_r)\text{sgn}(\omega)\pi/2} dV, \quad (6)$$

with the volume integration to be carried out over the variables \mathbf{x}' . In this equation

1. $\tau(\mathbf{x}', \mathbf{x}_s, \mathbf{x}_r)$ is the sum of the travel times from the source and receiver, respectively, to the output point:

$$\tau(\mathbf{x}, \mathbf{x}_s, \mathbf{x}_r) = \tau(\mathbf{x}, \mathbf{x}_s) + \tau(\mathbf{x}, \mathbf{x}_r), \quad (7)$$

with each of the separate travel times being solutions of the eikonal equation,

$$(\nabla\tau(\mathbf{x}, \mathbf{x}_0))^2 = \frac{1}{c^2(\mathbf{x})}, \quad \tau(\mathbf{x}_0, \mathbf{x}_0) = 0. \quad (8)$$

2. $a(\mathbf{x}', \mathbf{x}_s, \mathbf{x}_r)$ is a product of Green's function amplitudes,

$$a(\mathbf{x}, \mathbf{x}_s, \mathbf{x}_r) = A(\mathbf{x}, \mathbf{x}_s)A(\mathbf{x}, \mathbf{x}_r), \quad (9)$$

with the A 's a solution of the transport equation:

$$\nabla\tau(\mathbf{x}, \mathbf{x}_0) \cdot \nabla A(\mathbf{x}, \mathbf{x}_0) + A(\mathbf{x}, \mathbf{x}_0) \nabla^2 \tau(\mathbf{x}, \mathbf{x}_0) = 0, \quad \lim_{\mathbf{x} \rightarrow \mathbf{x}_0} A(\mathbf{x}, \mathbf{x}_0) |\mathbf{x} - \mathbf{x}_0| = \frac{1}{4\pi}. \quad (10)$$

3. $K(\mathbf{x}', \mathbf{x}_s, \mathbf{x}_r)$ is the sum of the *KMAH* indices for the ray trajectories from the source and the receiver to the point, \mathbf{x}' . This number counts the zeroes of the ray Jacobian or caustics of each of the ray fields from the source and receiver to \mathbf{x}' . The crossings produce phase shifts in the amplitude. The representation is invalid at those points where the caustic is right at one of the endpoints; we disregard these singular points in our further discussion.

2.3 Inversion.

Now, based on the representation of the forward model, above, we propose an inversion formula as follows:

$$\beta(\mathbf{x}, \theta) \sim \int i\omega W(\mathbf{x}, \hat{\nu}, \theta, \psi) u(\mathbf{x}_s(\mathbf{x}, \hat{\nu}, \theta, \psi), \mathbf{x}_r(\mathbf{x}, \hat{\nu}, \theta, \psi), \omega) \cdot e^{-i\omega\tau(\mathbf{x}, \mathbf{x}_s, \mathbf{x}_r) + iK(\mathbf{x}, \mathbf{x}_s, \mathbf{x}_r) \text{sgn}(\omega)\pi/2} d\alpha_1 d\alpha_2 d\omega d\psi. \quad (11)$$

In this equation, α_1 and α_2 are any parameters that define the unit sphere over which $\hat{\nu}$ ranges. In the expression, $u(\mathbf{x}_s(\mathbf{x}, \hat{\nu}, \theta, \psi), \mathbf{x}_r(\mathbf{x}, \hat{\nu}, \theta, \psi), \omega)$, the arguments of \mathbf{x}_s and \mathbf{x}_r emphasize the fact that for this integration, the source and receiver points are determined from the initial position at depth \mathbf{x} with the ray directions determined by the choices of $\hat{\nu}$, θ and ψ . Clearly, this holds for τ and K , as well. The additional arguments were omitted there for the sake of some brevity in the description.

The choice of travel time and *KMAH* index in this inversion is fairly standard and is known in other literature as phase matching: we have simply replaced the variable \mathbf{x}' of the modeling formula by the output variable \mathbf{x} and otherwise replaced the travel time and *KMAH* index of the modeling formula by their negatives for the purpose of inversion. Alternatively, when the inversion operator is viewed as a propagator, it can be seen to propagate the data back to its “zero time” as in a classic migration. For the moment, we have left the amplitude function fairly general except for the assumption that it does not depend on ω . This follows from knowledge of the corresponding weighting function for

common-offset, common shot and zero offset inversion. This will be verified below when we see that it results in the balancing of the powers of ω .

Finally, note that the ambiguity of the argument θ in the reflectivity, $\beta(\mathbf{x}, \theta)$, is resolved here. It is the prescribed opening angle of this common opening angle inversion dictated by the right side of the equation. Also, note that if we did not include an integration over ψ on the right side, then the left side would be $\beta(\mathbf{x}, \theta, \psi)$.

To learn more about W , we first substitute the result (6) for u into the inversion formula (11). The result is

$$\beta(\mathbf{x}, \theta) \sim \int_D \int \omega^2 F(\omega) \beta(\mathbf{x}', \theta) W(\mathbf{x}, \hat{\nu}, \theta, \psi) a(\mathbf{x}', \mathbf{x}_s, \mathbf{x}_r) \cdot e^{i\omega[\tau(\mathbf{x}', \mathbf{x}_s, \mathbf{x}_r) - \tau(\mathbf{x}, \mathbf{x}_s, \mathbf{x}_r)] + i[K(\mathbf{x}, \mathbf{x}_s, \mathbf{x}_r) - K(\mathbf{x}', \mathbf{x}_s, \mathbf{x}_r)] \text{sgn}(\omega) \pi/2} d\alpha_1 d\alpha_2 d\omega d\psi dV. \quad (12)$$

We see here that the integral over the \mathbf{x}' variables of the function $\beta(\mathbf{x}', \theta)$ times a rather complicated weighting function produces the function $\beta(\mathbf{x}, \theta)$. For this to occur, that complicated weighting function must be a Dirac delta function, at least asymptotically. In fact, this is plausible. Note that for $\mathbf{x}' = \mathbf{x}$, the phase is zero. Consequently, the integrand loses the oscillation that occurs for other choices of \mathbf{x}' . Thus, one should expect a larger result for the integration over the other variables for $\mathbf{x}' = \mathbf{x}$ than when $\mathbf{x}' \neq \mathbf{x}$. In the language of asymptotic expansions of integrals, the point $\mathbf{x}' = \mathbf{x}$ is a *critical point* of the integral.

Therefore, we write

$$\delta(\mathbf{x}' - \mathbf{x}) \sim \int_D \int \omega^2 F(\omega) W(\mathbf{x}, \mathbf{x}_s, \mathbf{x}_r) a(\mathbf{x}', \mathbf{x}_s, \mathbf{x}_r) |\nabla \tau(\mathbf{x}', \mathbf{x}_s, \mathbf{x}_r)| \cdot e^{i\omega[\tau(\mathbf{x}', \mathbf{x}_s, \mathbf{x}_r) - \tau(\mathbf{x}, \mathbf{x}_s, \mathbf{x}_r)] + i[K(\mathbf{x}, \mathbf{x}_s, \mathbf{x}_r) - K(\mathbf{x}', \mathbf{x}_s, \mathbf{x}_r)] \pi/2} d\alpha_1 d\alpha_2 d\omega d\psi. \quad (13)$$

Now let us approximate the integrand for \mathbf{x}' in the neighborhood of \mathbf{x} . In the amplitude and the K 's, that amounts to setting $\mathbf{x}' = \mathbf{x}$. while in the phase, we need the next term in a Taylor expansion, namely,

$$\omega[\tau(\mathbf{x}', \mathbf{x}_s, \mathbf{x}_r) - \tau(\mathbf{x}, \mathbf{x}_s, \mathbf{x}_r)] \sim \mathbf{k} \cdot (\mathbf{x}' - \mathbf{x}), \quad (14)$$

$$\mathbf{k} = \omega \nabla \tau(\mathbf{x}', \hat{\nu}, \theta)|_{\mathbf{x}' = \mathbf{x}} = \omega \nabla \tau(\mathbf{x}, \mathbf{x}_s, \mathbf{x}_r).$$

In accordance with the discussion below (11), we choose to make the identifications,

$$\begin{aligned} a(\mathbf{x}, \mathbf{x}_s, \mathbf{x}_r) &\Rightarrow a(\mathbf{x}, \hat{\nu}, \theta, \psi), & \nabla \tau(\mathbf{x}, \mathbf{x}_s, \mathbf{x}_r) &\Rightarrow \nabla \tau(\mathbf{x}, \hat{\nu}, \theta), \\ K(\mathbf{x}, \mathbf{x}_s, \mathbf{x}_r) &\Rightarrow K(\mathbf{x}, \hat{\nu}, \theta, \psi), & u(\mathbf{x}_s, \mathbf{x}_r, \omega) &\Rightarrow u(\hat{\nu}, \theta, \psi, \omega). \end{aligned} \quad (15)$$

From Figure 4, the gradient of the total travel time is in the direction of $\hat{\boldsymbol{\nu}}$. Furthermore, its magnitude depends on the opening angle, θ , but not on the angle ψ . In fact,

$$\nabla\tau(\mathbf{x}, \hat{\boldsymbol{\nu}}, \theta) = \frac{2 \cos \theta}{c(\mathbf{x})} \hat{\boldsymbol{\nu}}, \quad \rightarrow \quad \mathbf{k} = \frac{2\omega \cos \theta}{c(\mathbf{x})} \hat{\boldsymbol{\nu}}, \quad (16)$$

with $c(\mathbf{x})$ the wave speed at the output point \mathbf{x} . Thus, ψ is omitted from the argument of $\nabla\tau$ in the previous equation, even though the separate travel time gradients, $\nabla\tau(\mathbf{x}_s, \mathbf{x})$ and $\nabla\tau(\mathbf{x}_r, \mathbf{x})$ remain functions of ψ .

As with the derivation in Bleistein, et al., [2001], we see here that the source receiver configuration defines a local Fourier variable \mathbf{k} in terms of the frequency ω , the migration dip $\hat{\boldsymbol{\nu}}$, the opening angle θ and the wave speed $c(\mathbf{x})$. Further, we can see in (14) that the phase takes on the form familiar in Fourier transforms when expressed in terms of the new vector variable \mathbf{k} . Therefore, in (13) we propose to replace the integrations in the variables of $\hat{\boldsymbol{\nu}}$ and ω by a volume integral in \mathbf{k} as follows:

$$\begin{aligned} \delta(\mathbf{x}' - \mathbf{x}) \sim & \int_D \int \omega^2 F(\omega) W(\mathbf{x}, \hat{\boldsymbol{\nu}}, \theta, \psi) a(\mathbf{x}, \hat{\boldsymbol{\nu}}, \theta, \psi) |\nabla\tau(\mathbf{x}', \hat{\boldsymbol{\nu}}, \theta)| \\ & \cdot \left| \frac{\partial(\omega, \alpha_1, \alpha_2)}{\partial(\mathbf{k})} \right| e^{i\mathbf{k} \cdot (\mathbf{x}' - \mathbf{x})} d^3 k d\psi. \end{aligned} \quad (17)$$

In this equation, we have set $\mathbf{x}' = \mathbf{x}$ in the amplitude and in the K 's as mentioned above, including revising the arguments of a and $|\nabla\tau|$ from $\mathbf{x}_s, \mathbf{x}_r$ to $\hat{\boldsymbol{\nu}}, \theta, \psi$ as appropriate. Further, in the second line, we have introduced the absolute value of the Jacobian of transformation associated with the changed of variables that we have used. Note that this is merely a step along the way to the derivation of the proper weighting function, W . Once W is determined, it is formula (11) that is used to process data; we never have to derive expressions for ω and $\boldsymbol{\nu}$ in terms of \mathbf{k} . It is for this reason that we have not introduced a new notation for the amplitude as a function of \mathbf{k} .

In order to proceed, we need to know a little more about the nature of the Jacobian appearing in the second line of this last equation. Actually, it is easier for us to calculate the inverse of this Jacobian from the second line of (14). From that equation, we can see that

$$\frac{\partial(\mathbf{k})}{\partial(\omega, \alpha_1, \alpha_2)} = \omega^2 h(\mathbf{x}, \boldsymbol{\nu}, \theta), \quad (18)$$

with

$$h(\mathbf{x}, \boldsymbol{\nu}, \theta) = \det \begin{bmatrix} \nabla\tau(\mathbf{x}, \hat{\boldsymbol{\nu}}, \theta) \\ \frac{\partial\nabla\tau(\mathbf{x}, \hat{\boldsymbol{\nu}}, \theta)}{\partial\alpha_1} \\ \frac{\partial\nabla\tau(\mathbf{x}, \hat{\boldsymbol{\nu}}, \theta)}{\partial\alpha_2} \end{bmatrix}. \quad (19)$$

That is, $h(\mathbf{x}, \boldsymbol{\nu}, \theta)$ is just the Beylkin determinant, but now in the variables of integration of the migration dip. We caution the reader that this is a different use of the letter h than as the common-offset of earlier sections. Both uses of h are traditional in the literature. We will not return to the former use, so that the meaning of h should be clear in context; it is the 3D Beylkin determinant for the remainder of the paper.

Let us substitute this result into (17) to obtain

$$\delta(\mathbf{x}' - \mathbf{x}) \sim \int_D \int F(\omega) W(\mathbf{x}, \hat{\boldsymbol{\nu}}, \theta, \psi) \frac{a(\mathbf{x}, \hat{\boldsymbol{\nu}}, \theta, \psi) |\nabla\tau(\mathbf{x}', \hat{\boldsymbol{\nu}}, \theta)|}{|h(\mathbf{x}, \boldsymbol{\nu}, \theta)|} e^{i\mathbf{k}\cdot(\mathbf{x}' - \mathbf{x})} d^3k d\psi. \quad (20)$$

We want to compare this result with the exact distributional identity

$$\delta(\mathbf{x}' - \mathbf{x}) = \frac{1}{8\pi^3} \int e^{i\mathbf{k}\cdot(\mathbf{x}' - \mathbf{x})} d^3k.$$

In (20), we regard the function $F(\omega(\mathbf{k}))$ as providing band limiting in the radial direction in the \mathbf{k} -domain. Indeed, for full bandwidth, $F \equiv 1$. Thus, we can disregard this function for our present purposes. We propose, then, to choose W so that

$$W(\mathbf{x}, \hat{\boldsymbol{\nu}}, \theta, \psi) \frac{a(\mathbf{x}, \hat{\boldsymbol{\nu}}, \theta, \psi) |\nabla\tau(\mathbf{x}', \hat{\boldsymbol{\nu}}, \theta)|}{|h(\mathbf{x}, \boldsymbol{\nu}, \theta)|} \Psi = \frac{1}{8\pi^3}$$

or

$$W(\mathbf{x}, \hat{\boldsymbol{\nu}}, \theta, \psi) = \frac{1}{8\pi^3 \Psi} \frac{|h(\mathbf{x}, \boldsymbol{\nu}, \theta)|}{a(\mathbf{x}, \hat{\boldsymbol{\nu}}, \theta, \psi) |\nabla\tau(\mathbf{x}', \hat{\boldsymbol{\nu}}, \theta)|}. \quad (21)$$

In these two equations,

$$\Psi = \int d\psi, \quad (22)$$

where the range of integration is the coverage by source-receiver pairs on the acquisition surface for the given imaging point \mathbf{x} , migration dip $\hat{\boldsymbol{\nu}}$, opening angle θ and azimuths ψ . Essentially, with this normalization, the ψ -integral in (11) becomes an average of the contributions over all source-receiver pairs for which there are potentially specular returns. In

a discretization, the factor $\Delta\psi$ becomes irrelevant and one simply averages over the number of hits of nonzero data on the upper surface.

We will now simplify the above expression for W . First, we address the simplification of the Beylkin determinant, h in (21). First, \mathbf{k} in (16), we see that

$$h(\mathbf{x}, \boldsymbol{\nu}, \theta) = \left[\frac{2 \cos \theta}{c(\mathbf{x})} \right]^3 \det \begin{bmatrix} \hat{\boldsymbol{\nu}} \\ \frac{\partial \hat{\boldsymbol{\nu}}}{\partial \alpha_1} \\ \frac{\partial \hat{\boldsymbol{\nu}}}{\partial \alpha_2} \end{bmatrix} = \left[\frac{2 \cos \theta}{c(\mathbf{x})} \right]^3 \hat{\boldsymbol{\nu}} \cdot \frac{\partial \hat{\boldsymbol{\nu}}}{\partial \alpha_1} \times \frac{\partial \hat{\boldsymbol{\nu}}}{\partial \alpha_2}. \quad (23)$$

We now use (16) for $|\nabla\tau|$, (9) for a and this last result for $h(\mathbf{x}, \boldsymbol{\nu}, \theta)$ substituted into the expression for β , (11), to obtain

$$\beta(\mathbf{x}, \theta) = \frac{1}{4\pi^2\Psi} \left[\frac{2 \cos \theta}{c(\mathbf{x})} \right]^2 \int \frac{D_3(\mathbf{x}, \mathbf{x}_s, \mathbf{x}_r)}{A(\mathbf{x}, \mathbf{x}_s)A(\mathbf{x}, \mathbf{x}_r)} \left| \hat{\boldsymbol{\nu}} \cdot \frac{\partial \hat{\boldsymbol{\nu}}}{\partial \alpha_1} \times \frac{\partial \hat{\boldsymbol{\nu}}}{\partial \alpha_2} \right| d\alpha_1 d\alpha_2 d\psi \quad (24)$$

$$D_3(\mathbf{x}, \mathbf{x}_s, \mathbf{x}_r) = \frac{1}{2\pi} \int i\omega u(\mathbf{x}_s, \mathbf{x}_r, \omega) e^{-i\omega\tau(\mathbf{x}, \mathbf{x}_s, \mathbf{x}_r) + iK(\mathbf{x}, \hat{\boldsymbol{\nu}}, \theta, \psi) \text{sgn}(\omega)\pi/2} d\omega.$$

Through the inclusion of the *KMAH* index K , we account for phase shifts in the Green's functions due to caustics in their ray fields. There are only four distinct choices of K , 0,1,2,3. The case $K = 0$ yields minus the first derivative of the data, while $K = 2$ yields the derivative itself. Similarly, $K = 1$ yields the negative of the Hilbert transform of the first derivative of the data, and $K = 3$ yields the negative of this result. Hence, we need only two Fourier filtered inversions of the data in order to have data for all four choices of K .

Through the integration over azimuth ψ we include multi-azimuth data in the migration/inversion process. Had we not included the integration in ψ , then the final formula would be

$$\beta(\mathbf{x}, \theta, \psi) = \frac{1}{4\pi^2} \left[\frac{2 \cos \theta}{c(\mathbf{x})} \right]^2 \int \frac{D_3(\mathbf{x}, \mathbf{x}_s, \mathbf{x}_r)}{A(\mathbf{x}, \mathbf{x}_s)A(\mathbf{x}, \mathbf{x}_r)} \left| \hat{\boldsymbol{\nu}} \cdot \frac{\partial \hat{\boldsymbol{\nu}}}{\partial \alpha_1} \times \frac{\partial \hat{\boldsymbol{\nu}}}{\partial \alpha_2} \right| d\alpha_1 d\alpha_2. \quad (25)$$

This method still does not include an accurate accommodation of the case in which the caustic of the rays from source or receiver is right at the output point \mathbf{x} , but then, neither does more standard Kirchhoff inversion. Further, we would argue that in this special case, the usual interpretation of the output in terms of reflectivity makes no sense either. The reflection coefficient is a concept from plane wave reflection. It has relevance in ray theory,

away from caustics, only to the extent that the wave fronts in this case are locally planar on the scale of a wave length (high-frequency assumption). In the neighborhood of a caustic, that local plane wave structure is no longer valid. Thus, the method breaks down (weakly) at points where simple ray theory is no longer valid. On the other hand, the proposed method extends the utility of Kirchhoff migration-inversion beyond the standard implementations for the common shot or common-offset case.

Recall Bleistein, et al., [2001], that on the peak of the reflector, the theory predicts that

$$\beta_{\text{peak}}(\mathbf{x}, \theta) = R(\mathbf{x}, \theta) \frac{2 \cos \theta}{c(\mathbf{x})} \frac{1}{2\pi} \int F(\omega) d\omega,$$

for each specular source-receiver pair. The integration over ψ provides an average of such peak values at the same θ , thus possibly improving the resulting estimate of $R(\mathbf{x}, \theta$ at the fixed value of θ .

Remark

Equation (23) is the extension to 3D of the 2D result (1) stated in the introduction. It is a general result about the Beylkin determinant that follows from the representation of \mathbf{k} in (16), which is also a general result. Note that

$$\left| \hat{\nu} \cdot \frac{\partial \hat{\nu}}{\partial \alpha_1} \times \frac{\partial \hat{\nu}}{\partial \alpha_2} \right| d\alpha_1 d\alpha_2 = dS,$$

with dS the differential area element on the unit sphere. This is completely analogous to the 2D case in which one of the roles of H was to provide the appropriate scaling to transform the integration with respect to an arbitrary parameter into an integral with respect to arc length. Thus, the triple scalar product or determinant is seen to be the ratio of differential area elements in a parameter domain in (α_1, α_2) and the image of that domain on the unit sphere in $\hat{\nu}$. The common-offset Beylkin determinant in 3D is particularly onerous to compute analytically. We see now that the difficulty is one of relating the midpoint and azimuth of a source receiver pair to migration dip direction at depth. Albertin et al., [1999], have provided a computational technique for estimating this determinant. That method involves shooting rays in a regular grid on a patch in (α_1, α_2) and counting the number of hits in an image patch on the unit sphere.

Any further simplification requires us finally to define the parameters α_1 and α_2 with which we describe the vector $\hat{\nu}$ and with respect to which we will ultimately integrate to define the inversion operator. We have two good choices here, polar coordinates and cylindrical coordinates.

2.4 Polar Coordinates.

The most straightforward choice for these variables are the standard polar angles measured from the point \mathbf{x} , as depicted in Figure 6. In terms of these coordinates, we can write

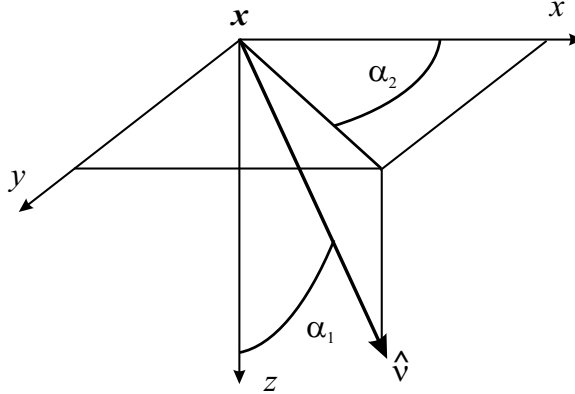


Figure 6: Polar coordinates α_1 and α_2 used to define the vector $\hat{\nu}$.

$$\hat{\nu} = (\sin \alpha_1 \cos \alpha_2, \sin \alpha_1 \sin \alpha_2, \cos \alpha_1) \quad (26)$$

and carry out the differentiations in (23) to find that

$$h(\mathbf{x}, \boldsymbol{\nu}, \theta) = \left[\frac{2 \cos \theta}{c(\mathbf{x})} \right]^3 \sin \alpha_1. \quad (27)$$

We use this result in (24) to obtain

$$\beta(\mathbf{x}, \theta) = \frac{1}{8\pi^3 \Psi} \left[\frac{2 \cos \theta}{c(\mathbf{x})} \right]^2 \int \frac{D_3(\mathbf{x}, \mathbf{x}_s, \mathbf{x}_r)}{A(\mathbf{x}, \mathbf{x}_s)A(\mathbf{x}, \mathbf{x}_r)} \sin \alpha_1 d\alpha_1 d\alpha_2 d\psi. \quad (28)$$

2.5 Cylindrical Coordinates.

This second choice was suggested by Y. Zhang. We use the x axis and the polar angle for y and z , as suggested in Figure 7. In this case,

$$\hat{\nu} = (\alpha_1, \sqrt{1 - \alpha_1^2} \cos \alpha_2, \sqrt{1 - \alpha_1^2} \sin \alpha_2), \quad (29)$$

and the determinant in (23) is equal to one. Therefore, the reflectivity in this case becomes

$$\beta(\mathbf{x}, \theta) = \frac{1}{4\pi^2 \Psi} \left[\frac{2 \cos \theta}{c(\mathbf{x})} \right]^2 \int \frac{D_3(\mathbf{x}, \mathbf{x}_s, \mathbf{x}_r)}{A(\mathbf{x}, \mathbf{x}_s)A(\mathbf{x}, \mathbf{x}_r)} d\alpha_1 d\alpha_2 d\psi \quad (30)$$

This completes our discussion of the 3D case.

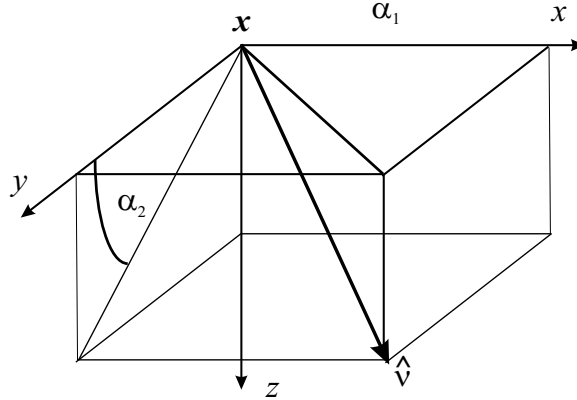


Figure 7: Cylindrical coordinates α_1 and α_2 used to define the vector $\hat{\mathbf{v}}$.

3 Formulas in 2D and 2.5D

We provide the inversion formulas corresponding to (24) in 2D and 2.5D without derivation. The 2D inversion allows a comparison with the result of Xu et al., [2001]. Two-and-one-half-dimensions (2.5D), inversion allows processing of a single line of data in a 3D environment. It properly takes account of three-dimensional propagation in the background medium, but assumes no earth variation in the out-of-plane direction—essentially, a 2D earth. This is appropriate in practice when the single line survey is carried out in the dip direction.

For 2D, the result is

$$\beta(\mathbf{x}, \theta) = \frac{1}{2\pi} \frac{2 \cos \theta}{c(\mathbf{x})} \int \frac{D_2(\mathbf{x}, \mathbf{x}_s, \mathbf{x}_r)}{A(\mathbf{x}, \mathbf{x}_s)A(\mathbf{x}, \mathbf{x}_r)} d\phi, \quad (31)$$

$$D_2(\mathbf{x}, \mathbf{x}_s, \mathbf{x}_r) = \frac{1}{2\pi} \int |\omega| d\omega e^{-i\omega\tau(\mathbf{x}, \mathbf{x}_s, \mathbf{x}_r) + iK(\mathbf{x}, \mathbf{x}_s, \mathbf{x}_r) \operatorname{sgn}(\omega)\pi/2} u_S(\mathbf{x}_s, \mathbf{x}_r, \omega).$$

Here, the A 's are ray-theoretic 2D Green's function amplitudes. This formula agrees with the implicit inversion for reflectivity in Xu et al., [2002].

For 2.5D, the corresponding formula is

$$\beta(\mathbf{x}, \theta) = \frac{1}{[2\pi]^{3/2}} \int \frac{\sqrt{\sigma_s + \sigma_r} D_{2.5}(\mathbf{x}, \mathbf{x}_s, \mathbf{x}_r)}{A_2(\mathbf{x}, \mathbf{x}_s)A_2(\mathbf{x}, \mathbf{x}_r)} d\phi, \quad (32)$$

$$D_{2.5}(\mathbf{x}, \mathbf{x}_s, \mathbf{x}_r) = \frac{1}{2\pi} \frac{2 \cos \theta}{c(\mathbf{x})} \int \sqrt{|\omega|} d\omega e^{-i\omega\tau(\mathbf{x}, \mathbf{x}_s, \mathbf{x}_r) + i[\pi/4 + K(\mathbf{x}, \mathbf{x}_s, \mathbf{x}_r)\pi/2] \operatorname{sgn}(\omega)} u_S(\mathbf{x}_s, \mathbf{x}_r, \omega).$$

4 Summing over Sources and Receivers.

While the theoretical results presented above might seem attractive, there are serious problems in numerical implementation. First, sorting ray trajectories is more difficult from the bottom up than from the top down. Second, ray arrivals at the upper surface will sample the traces more sparsely at shallow take-off angles than at steep angles, perhaps introducing aliasing problems. This provides substantive justification to seek a technique for implementing this migration-inversion in common opening angle as a sum over source-receiver pairs at the upper surface.

Let us think in the continuous 2D case for the present. We might think to integrate over all traces for which the ray trajectory from source and receiver intersect at the output point \mathbf{x} . The data at the appropriate travel time would then sample all dips available in the data set, but it would also sample all opening angles available in the data set. Thus, we need a mechanism that allows us to restrict the source-receiver pairs to those with the common opening angle. Further, we need a way to transform the formula in (31), which is a 1D integration into an integral over two variables labeling the source and receiver positions along a line. Luckily, we can accomplish both of these objectives by the simple device of introducing an integral over opening angle in (31) and then introducing a Dirac delta function to restrict that angle to the fixed θ of the cited equation. That is, we rewrite (31) as

$$\beta(\mathbf{x}, \theta) = \frac{1}{2\pi} \frac{2 \cos \theta}{c(\mathbf{x})} \int \frac{D_2(\mathbf{x}, \mathbf{x}_s, \mathbf{x}_r)}{A(\mathbf{x}, \mathbf{x}_s)A(\mathbf{x}, \mathbf{x}_r)} \delta(\theta' - \theta) d\phi d\theta'. \quad (33)$$

Now we are prepared to make a change of variables of integration from ϕ and θ to r and s , the parameters that label the positions of \mathbf{x}_r and \mathbf{x}_s , respectively. For example, if the acquisition surface were horizontal, we could set $\mathbf{x}_s = (s, 0)$ and $\mathbf{x}_r = (r, 0)$, but we can allow for a more general upper surface, as well. Without worrying about the singular behavior of the change of variables for the moment, then, we set

$$\beta(\mathbf{x}, \theta) = \frac{1}{2\pi} \frac{2 \cos \theta}{c(\mathbf{x})} \int \frac{D_2(\mathbf{x}, \mathbf{x}_s, \mathbf{x}_r)}{A(\mathbf{x}, \mathbf{x}_s)A(\mathbf{x}, \mathbf{x}_r)} \delta(\theta' - \theta) \left| \frac{\partial(\theta' \phi)}{\partial(r, s)} \right| dr ds. \quad (34)$$

This is Xu et al.'s, [2000] equation (35). We see here an integration over all sources and receivers restricted by the Dirac delta function to include only contributions for which the opening angle of the rays at the output point \mathbf{x} is equal to θ . Of course, in the discrete application, the delta function will be allowed to act in some range, $\pm\Delta\theta/2$ around θ . Similarly, the included rays will pass through an appropriate sized cell around the point \mathbf{x} .

The Jacobian in this equation becomes infinite when \mathbf{x}_s or \mathbf{x}_r is on a caustic of the rays from \mathbf{x} . However, here one or the other Green's function amplitudes is infinite, as well.

Recall, however, that these amplitudes are incorrect at such points. For smooth caustics, nevertheless, the resulting singularity is integrable. If, such a point arose in a discrete sum, the integrand could be replaced by zero without seriously affecting the result. We only lose information for amplitude and location at the reflection point for which this distinguished ray is part of the specular ray pair.

4.1 Simplifying the Jacobian in (34).

Here, we examine further the nature of the Jacobian appearing in (34). First, we observed earlier that for each migration dip γ at \mathbf{x} there is a single point \mathbf{x}_0 where the ray emerges on the acquisition surface. Further, for an acquisition curve, the point \mathbf{x}_0 is defined by a single parameter, say q , $\mathbf{x}_0 = \mathbf{x}_0(q)$, so that q is a single valued function of γ for a given \mathbf{x} . That is,

$$q = f(\gamma, \mathbf{x}).$$

The choices, r and s , are particular values of γ . In fact,

$$s = f(\gamma, \mathbf{x})|_{\gamma=\phi \mp \theta'} = f(\phi \mp \theta', \mathbf{x}), \quad r = f(\gamma, \mathbf{x})|_{\gamma=\phi \pm \theta'} = f(\phi \pm \theta', \mathbf{x}). \quad (35)$$

Furthermore, under rather mild conditions on the ray equations, including differentiability of the background wave speed, f is a differentiable function of γ .

To obtain an expression for the Jacobian in (34), we need to differentiate the previous equation with respect to θ' and ϕ .

$$\frac{\partial s}{\partial \phi} = \frac{\partial f(\gamma, \mathbf{x})}{\partial \gamma} \Big|_{\gamma=\phi \mp \theta'} = f_\gamma(\phi \mp \theta', \mathbf{x}), \quad \frac{\partial s}{\partial \theta'} = \mp f_\gamma(\phi \mp \theta', \mathbf{x}), \quad (36)$$

$$\frac{\partial r}{\partial \phi} = f_\gamma(\phi \pm \theta', \mathbf{x}), \quad \frac{\partial r}{\partial \theta'} = \pm f_\gamma(\phi \pm \theta', \mathbf{x})$$

Using these results, it follows that

$$\left| \frac{\partial(s, r)}{\partial(\theta', \phi)} \right| = |f_\gamma(\phi \mp \theta', \mathbf{x}) f_\gamma(\phi \mp \theta', \mathbf{x})| = |f_\gamma(\phi + \theta', \mathbf{x}) f_\gamma(\phi - \theta', \mathbf{x})|, \quad (37)$$

in which case

$$\left| \frac{\partial(\theta', \phi)}{\partial(s, r)} \right| = \frac{1}{|f_\gamma(\phi + \theta', \mathbf{x}) f_\gamma(\phi - \theta', \mathbf{x})|}. \quad (38)$$

This equation is equivalent to Xu et al.'s [2000] equation (37), since their $\beta_s = \pi - (\phi \mp \theta')$ and their $\beta_r = \pi - (\phi \pm \theta')$. However, whereas they claim that their (37) is approximate, we

see here that their result and ours are exact. With this in place, (34) agrees with Xu et al.'s [2000] equation (35) for the reflectivity as an inversion in dip for constant opening angle, but performed as an integral over all sources and receivers.

4.2 Summing over sources and receivers in 3D.

In 3D, the source and receiver are each a function of two parameters, (s_1, s_2) and (r_1, r_2) respectively. Now, the arrival of a ray at the upper surface is a single valued function of the four variables, $(\alpha_1, \alpha_2, \theta, \psi)$. Thus, in analogy with the 2D case, we now rewrite the 3D inversion formula (25) as the following fourfold integral

$$\beta(\mathbf{x}, \theta, \psi) = \frac{1}{4\pi^2} \left[\frac{2 \cos \theta}{c(\mathbf{x})} \right]^2 \int \frac{D_3(\mathbf{x}, \mathbf{x}_s, \mathbf{x}_r)}{A(\mathbf{x}, \mathbf{x}_s)A(\mathbf{x}, \mathbf{x}_r)} \left| \hat{\mathbf{v}} \cdot \frac{\partial \hat{\mathbf{v}}}{\partial \alpha_1} \times \frac{\partial \hat{\mathbf{v}}}{\partial \alpha_2} \right| \cdot \delta(\theta' - \theta) \delta(\psi' - \psi) d\alpha_1 d\alpha_2 d\theta' d\psi'. \quad (39)$$

Now we can introduce the transformation to surface coordinates (s_1, s_2, r_1, r_2) to obtain

$$\beta(\mathbf{x}, \theta, \psi) = \frac{1}{4\pi^2} \left[\frac{2 \cos \theta}{c(\mathbf{x})} \right]^2 \int \frac{D_3(\mathbf{x}, \mathbf{x}_s, \mathbf{x}_r)}{A(\mathbf{x}, \mathbf{x}_s)A(\mathbf{x}, \mathbf{x}_r)} \left| \hat{\mathbf{v}} \cdot \frac{\partial \hat{\mathbf{v}}}{\partial \alpha_1} \times \frac{\partial \hat{\mathbf{v}}}{\partial \alpha_2} \right| \cdot \delta(\theta' - \theta) \delta(\psi' - \psi) \left| \frac{\partial(\alpha_1, \alpha_2, \theta', \psi')}{\partial(s_1, s_2, r_1, r_2)} \right| ds_1 ds_2 dr_1 dr_2. \quad (40)$$

Unfortunately, the Jacobian appearing in this equation does not lend itself to a simplification analogous to the result in 2D. Thus, to carry out a common opening angle inversion in terms of surface variables in 3D we are again faced with having a daunting computation for the Beylkin determinant.

5 Summary and Conclusions.

We have presented a derivation of 3D migration-inversion as an integration in migration dip. This is a common (constant) opening angle method as contrasted with common-offset migration-inversion. It assures a peak output that is proportional to the reflection coefficient at the known opening angle on each panel of the output and leads directly to an AVA graph from the moveout in angle panels. The derivation follows the same classical lines as in previous Kirchhoff inversions, thereby placing this method in the same class as earlier

such inversions. We have presented the corresponding results in 2D and 2.5D making comparison with earlier 2D results derived via the least squares method. Papers that derive this type of inversion via the generalized Radon transform technique do not provide acoustic inversion formulas for comparison. We believe that the derivation here is more accessible to the geophysical community. We have pointed out that the Beylkin determinant can be interpreted as a second power (in 2D) or third power (in 3D) of the magnitude of the travel time gradient multiplied by the derivative of the migration dip (in 2D) or the rate of change of the migration dip solid angle (in 3d) with respect to the parameters of integration in the inversion operator. This result has been known in various guises and is the basis for computing the Beylkin determinant in terms of hit counts of ray directions as a function of integration parameters.

References

- Albertin, U., and H. Jaramillo, D. Yingst, R. Bloor, W. Chang, C. Beasley, E. Mobley, 1999, Aspects of true amplitude migration: Expanded Abstracts, International Meeting of the Society of Exploration Geophysicists, Houston, 1358-1361.
- Bleistein, N., J. K. Cohen and J. W. Stockwell, Jr., 2001, *Mathematics of Multidimensional Seismic Imaging, Migration and Inversion*: Springer-Verlag, New York.
- Červený, V., 1995, Seismic wave fields in three-dimensional isotropic and anisotropic structures. Lecture Notes, University of Trondheim, Norway.
- Červený, V., 2001, *Seismic Ray Theory*. Cambridge University Press, Cambridge.
- Kravtsov, Yu. A., and Yu. I. Orlov, 1990, *Geometrical Optics of Inhomogeneous Media*. Springer-Verlag, New York.
- de Hoop, M. V., 1998. Asymptotic inversion: multipathing and caustics. Sixty-eighth International Meeting of the Society of Exploration Geophysicists, Expanded abstracts, SEG, Tulsa, 1534–1537.
- de Hoop, M. V. and S. Brandesberg-Dahl, 2000. Maslov asymptotic extension of generalized Radon transform inversions in anisotropic elastic media: A least-squares approach: *Inverse Problems*, 16, no. 3, 519-562.
- Xu, S. H. Chauris, G. Lambaré and M. S. Noble, 2001, Common-angle migration: A strategy for imaging complex media: *Geophysics*, 66, 6, 1877-1894.